

Polymerizable Lyotropic Liquid Crystals Containing Transition-Metal Ions as Building Blocks for Nanostructured Polymers and Composites

David H. Gray and Douglas L. Gin*

Department of Chemistry, University of California, Berkeley, California 94720-1460

Received December 31, 1997. Revised Manuscript Received May 1, 1998

Transition-metal-containing analogues of a polymerizable lyotropic liquid crystal were prepared from sodium *p*-styryloctadecanoate by ion exchange with water-soluble metal chlorides, nitrates, and acetates. The mesophases of these amphiphilic monomers were investigated by polarized light microscopy, low-angle X-ray diffraction, and infrared spectroscopy. It was found that cadmium(II), manganese(II), and cobalt(II) *p*-styryloctadecanoate form an inverted hexagonal lyotropic phase at ambient temperature (22 °C), while the copper(II) salt forms a columnar hexagonal thermotropic phase. The monomers can be cross-linked photolytically in their respective liquid crystal phases with retention of phase architecture to yield polymer networks containing ordered microdomains of transition-metal ions. The relationship between the dimensions of the hexagonal mesophase formed and the identity of the counterion present in each salt is discussed. The polymerized inverted hexagonal phase of the cadmium salt was also used as a template for the formation of CdS nanoparticles, affording a novel, nanostructured composite.

Introduction

The design and preparation of synthetic materials with architectural control on the nanometer scale is an active area of research interest.¹ Biological structural materials have been used as models for the development of novel composites, since these materials derive their unique physical properties from the ordered meshing of organic and inorganic components. Bone,² for example, is composed of hydroxyapatite crystals integrated into an ordered collagen matrix. The process by which such biological materials are produced is referred to as biomineralization,^{3–5} whereby an organic medium acts as a backdrop for the ordered assembly of inorganic components. The extent of small-scale architectural control that this templating method can achieve has recently been applied to synthetic composites to afford new materials with interesting and tunable properties. Several approaches have been successful in controlling order on the nanometer size regime,^{6,7} including the use of Langmuir–Blodgett and self-assembled films,⁸ mineralization within lipid templates,⁹ the growth of organic

polymers in layered inorganic structures¹⁰ and zeolites,¹¹ the formation of nanoclusters within block copolymers,^{12–14} and the condensation of sol–gel materials within amphiphilic environments to form mesoporous sieves.^{15–17}

Recently, we developed a novel approach to forming nanocomposites with hexagonal symmetry by exploiting the self-assembling properties of polymerizable, ionic amphiphiles.¹⁸ In this process, a lyotropic liquid-crystalline (LC) mixture consisting of a polymerizable mesogen and reactive hydrophilic precursors spontaneously organizes into an inverse hexagonal mesophase (Scheme 1). The mixture is subsequently photopolymerized, forming a heavily cross-linked network around the precursor solution and locking the structure of the matrix into place. This organic matrix then acts as a template which directs the formation of a “filler” material within the hydrophilic channels. The reactions that form the polymer network and the filler material can occur either simultaneously or sequentially, depending on the method of initiation used for the reactions. We

(1) For examples of recent reviews, see: (a) Ozin, G. A. *Adv. Mater.* **1992**, *4*, 612. (b) Bein, T. *Chem. Mater.* **1996**, *8*, 1636. (c) Wen, J.; Wilkes, G. L. *Chem. Mater.* **1996**, *8*, 1667. (d) Calvert, P.; Ricke, P. *Chem. Mater.* **1996**, *8*, 1715. (e) Martin, C. R. *Chem. Mater.* **1996**, *8*, 1739. (f) Sayari, A. *Chem. Mater.* **1996**, *8*, 1840.

(2) Katz, E. P.; Wachtel, E.; Yamaughi, M.; Mechanic, G. L. *Connect. Tissue Res.* **1989**, *21*, 149.

(3) Mann, S. *Nature* **1993**, *365*, 499.

(4) Addadi, L.; Weiner, S. *Angew. Chem., Int. Ed. Engl.* **1992**, *31*, 153.

(5) Heywood, B. R.; Mann, S. *Adv. Mater.* **1994**, *6*, 9.

(6) Calvert, P. *Mater. Res. Soc. Bull.* **1992**, *17*, 37.

(7) Heuer, A. H.; Fink, D. J.; Laraia, V. J.; Arias, J. L.; Calvert, P. D.; Kendall, K.; Messing, G. L.; Blackwell, J.; Rieke, P. C.; Thompson, D. H.; Wheller, A. P.; Veis, A.; Caplan, A. I. *Science* **1992**, *255*, 1098.

(8) Fendler, J. H. *Chem. Mater.* **1996**, *8*, 1616.

(9) Archibald, D. D.; Mann, S. *Nature* **1993**, *364*, 430.

(10) Okada, A.; Usuki, A. *Mater. Sci. Eng.* **1995**, *C3*, 109.

(11) Frisch, H. L.; Mark, J. E. *Chem. Mater.* **1996**, *8*, 1735.

(12) Sohn, B. H.; Cohen, R. E. *Chem. Mater.* **1997**, *9*, 264.

(13) Ng Cheong Chan, Y.; Craig, G. S. W.; Schrock, R. R.; Cohen, R. E. *Chem. Mater.* **1992**, *4*, 885.

(14) Ng Cheong Chan, Y.; Schrock, R. R.; Cohen, R. E. *J. Am. Chem. Soc.* **1992**, *114*, 7295.

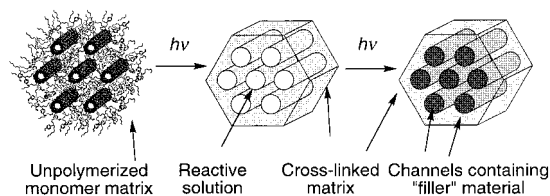
(15) Beck, J. S.; Vartuli, J. C.; Roth, W. J.; Leonowicz, M. E.; Kresge, C. T.; Schmitt, K. D.; Chu, C. T.-W.; Olson, D. H.; Sheppard, E. W.; McCullen, S. B.; Higgins, J. B.; Schlenker, J. L. *J. Am. Chem. Soc.* **1992**, *114*, 10834.

(16) Judeinstein, P.; Sanchez, C. *J. Mater. Chem.* **1996**, *6*, 511.

(17) Raman, N. K.; Anderson, M. T.; Brinker, C. J. *Chem. Mater.* **1996**, *8*, 1682.

(18) Gray, D. H.; Hu, S.; Juang, E.; Gin, D. L. *Adv. Mater.* **1997**, *9*, 731.

Scheme 1. Synthesis of Hexagonal Nanocomposites Using Lyotropic Liquid Crystal Monomers



have applied this approach to the preparation of nanostructured composites incorporating both inorganic and organic materials, such as sol-gel silica and poly(*p*-phenylenevinylene).¹⁹ We have also demonstrated that the resulting nanocomposites display unique physical properties due to the environment within the template.

After preparing these initial composites, we wished to expand the potential of our templating method by altering the spatial dimensions of the mesophase and incorporating different filler materials such as semiconductors. Lyotropic liquid crystals (LLCs) are known to arrange in several geometries, including micelles, lamellae, and columns, depending on the structure and functionality of the amphiphile used, the concentration of additives or solvents, and the temperature of the system. The mesophase that a LLC mixture will adopt at a fixed temperature and composition depends heavily on the shape of the mesogen itself.^{20–22} Israelachvili et al. formulated an expression termed the “critical packing parameter”, $Q = v/a_0l_c$, which relates the ratio of the volume of the organic portion of the mesogen (v), the area of the amphiphilic headgroup (a_0), and average critical length (l_c) to the expected curvature of the various mesophases. Mesogens with a comparatively large headgroup area and small organic volume, or $Q \leq 1$, are thought to favor “regular” micelles or columns, wherein the organic components resides within the interior of the structure. In contrast, mesogens with a small headgroup and large organic volume, or $Q > 1$, favor the corresponding “inverted” structures. Excluding temperature and solvent effects, the phase formed by a particular LLC can thus be altered by either changing the structure of the hydrophobic portion of the monomer or by altering the hydrophilic headgroup.

To most rapidly extend the physical properties exhibited by our template system, we chose to alter the ionic headgroup of our LLC monomer by preparing transition-metal analogues. We thought that incorporation of transition-metal ions into the parent amphiphile system would produce a new set of lyotropic metallomesogen templates with which we might have the ability (1) to modulate the dimensions of the mesophase by variation of the metal counterion; (2) to incorporate new physical properties associated with the metal ions, such as altered fluorescence, optical, or magnetic behavior; and (3) to provide a new chemical environment within the hydrophilic channels as the basis for forming different inorganic materials in situ. Modulation of the geometry and dimensions of lyotropic mesophases

through counterion substitution has previously been demonstrated in an ionic LLC.²³ Calcium²⁴ and cadmium²⁵ salts of identical saturated straight-chain carboxylic acids have been shown by low-angle X-ray diffraction to display inverse hexagonal phases with different interchannel spacings. Extensive research has been devoted to thermotropic metallomesogens²⁶ and, more recently, their polymerizable analogues.²⁷ However, very little if any work has been published in the area of polymerizable amphiphiles containing transition-metal ions and their ability to form organized polymer assemblies. Herein, we report the synthesis, polymerization, and initial characterization of a series of transition-metal LLCs and a new inorganic-organic composite prepared using this approach.

Experimental Section

General. ¹H NMR spectra were measured on a Bruker AMX-300 spectrometer. Chemical shifts are reported in ppm relative to residual nondeuterated solvent (CHCl₃ δ = 7.26; CH₃OH δ = 4.87). Multiplicities are given as s (singlet) and m (multiplet). IR spectra of the neat salts and polymerization mixtures were taken using a Perkin-Elmer 1616 series FT-IR as thin films on Ge crystals at ambient temperature. Ambient temperature X-ray diffraction spectra were taken using an Inel CPS 120 position-sensitive detector employing Cu K α radiation. X-ray diffraction samples were typically thin-film samples prepared on aluminum disks. Optical textures were obtained using a Leica DMRXP polarized light microscope equipped with a Wild MPS 48/52 automatic camera assembly. UV-visible absorption measurements were performed using a Hewlett-Packard HP 8425A spectrophotometer on samples prepared on quartz disks. Elemental analyses were performed at Galbraith Laboratories Inc., Knoxville, TN. LC samples were centrifuged in an IEC Centra CL2 centrifuge and sonicated in a Fisher Scientific FS14 sonicator. A Cole-Palmer 9815 series 6 W UV (365 nm) lamp was used for photopolymerization; UV flux measurements were taken with a Spectroline DRC-100X digital radiometer equipped with a DIX-365 UV-A sensor.

All chemicals and solvents were reagent grade and used as obtained without further purification. *n*-Pentane, ethanol (denatured), sodium hydroxide, and potassium hydroxide were purchased from Fisher Scientific. Cobalt(II) nitrate hexahydrate, manganese(II) chloride tetrahydrate, copper(II) acetate monohydrate, and cadmium chloride were purchased from the Aldrich Chemical Co. Calcium nitrate tetrahydrate was purchased from Mallinckrodt.

***p*-Styryloctadecanoic Acid (1).** The parent acid was synthesized according to literature procedures, and characterization data were consistent with those reported for the compound.¹⁸ ¹H NMR (CDCl₃, 300 MHz): δ 7.35–7.08 (4H, aromatic H), 6.71 (1H, CH₂=CHR, J_{trans} = 17.7 Hz, J_{cis} = 10.8), 5.72 (1H, CH_{trans}H_{cis}=CHR, J_{trans} = 17.55 Hz, J_{gem} = 1.05 Hz), 5.19 (1H, CH_{trans}H_{cis}=CHR, J_{cis} = 10.95 Hz, J_{gem} = 0.75 Hz), 2.47 (m, 1H, RCHPhR), 2.29 (m, 2H, RCH₂COOCH₃), 1.59 (m, 6H), 1.22 (m, 22H), 0.87 (m, 3H, RCH₃). IR: 1710 (C=O), 1630 (C=C), 989 (C=C), 902 (C=C), 838 (*p*-substituted phenyl) cm⁻¹. Anal. Calcd for C₂₆H₄₂O₂: C, 80.77; H, 10.95. Found: C, 80.63; H, 10.86.

(23) Herz, J.; Reiss-Husson, F.; Rempp, P.; Luzzati, V. *J. Polym. Sci., Part C* **1963**, *4*, 1275.

(24) Spegt, P. A.; Skoulios, A. E. *Acta Crystallogr.* **1964**, *17*, 198.

(25) Spegt, P. A.; Skoulios, A. E. *Acta Crystallogr.* **1963**, *16*, 301.

(26) For recent reviews on thermotropic metallomesogens, see: (a) Espinet, P.; Esteruelas, M. A.; Oro, L. A.; Serrano, J. L.; Sola, E. *Coord. Chem. Rev.* **1992**, *117*, 215. (b) Hudson, S. A.; Maitlis, P. M. *Chem. Rev.* **1993**, *93*, 861. (c) Neve, F. *Adv. Mater.* **1996**, *8*, 277.

(27) (a) Van der Pol, J. F.; Neeleman, E.; van Miltenburg, J. C.; Swikker, J. W.; Nolte, R. J. M.; Drenth, W. *Macromolecules* **1990**, *23*, 155. (b) Attard, G. S.; Templer, R. H. *J. Mater. Chem.* **1993**, *3*, 207. (c) Marcot, L.; Maldivi, P.; Marchon, J.-C.; Guillon, D.; Mohammed, I.-E.; Broer, D. J.; Mol, G. N. *Chem. Mater.* **1997**, *9*, 2051.

(19) Smith, R. C.; Fischer, W. M.; Gin, D. L. *J. Am. Chem. Soc.* **1997**, *119*, 4092.

(20) Seddon, J. M. *Biochim. Biophys. Acta* **1990**, *1031*, 1.

(21) Israelachvili, J. N.; Marcelija, S.; Horn, R. *Q. Rev. Biophys.* **1980**, *13*, 121.

(22) Gruen, D. W. R. *J. Phys. Chem.* **1985**, *89*, 146.

Sodium *p*-Styryloctadecanoate (2). In a 50-mL Erlenmeyer flask, 0.500 g (1.29 mmol) of acid **1** was dispersed in 20 mL of absolute ethanol. A stock solution of 0.155 M aqueous sodium hydroxide was prepared by dissolving 0.621 g (15.5 mmol) of sodium hydroxide in 100.0 mL of deionized water. Compound **1** was neutralized by adding 8.4 mL (1.3 mmol) of the NaOH solution slowly with stirring. The solution turned slightly cloudy at the start of addition and then cleared rapidly. The solvents were removed slowly by a rotary evaporator, and the sample was dried in vacuo for 12 h. The resulting product (0.424 g, 80%) was a white, sticky, flaky solid. $^1\text{H NMR}$ (CD_3OD , 300 MHz): δ 7.31–7.05 (4H, aromatic H), 6.68 (1H, $\text{CH}_2=\text{CHR}$, $J_{\text{trans}} = 17.6$ Hz, $J_{\text{cis}} = 11.1$), 5.69 (1H, $\text{CH}_{\text{trans}}\text{H}_{\text{cis}}=\text{CHR}$, $J_{\text{trans}} = 17.4$ Hz), 5.13 (1H, $\text{CH}_{\text{trans}}\text{H}_{\text{cis}}=\text{CHR}$, $J_{\text{cis}} = 10.8$ Hz), 2.45 (m, 1H, RCHPhR), 2.12 (m, 2H, $\text{RCH}_2\text{-COOCH}_3$), 1.54 (m, 6H), 1.22 (m, 22H), 0.96 (m, 3H, RCH_3). IR: 1630 (C=C), 1564 (COO^-), 988 (C=C), 902 (C=C), 838 (*p*-substituted phenyl) cm^{-1} . Anal. Calcd for $\text{C}_{26}\text{H}_{41}\text{O}_2\text{Na}$: C, 76.43; H, 10.11; Na, 5.63. Found: C, 75.22; H, 10.24.

Potassium *p*-styryloctadecanoate (3) was prepared by the same method as above, from 0.0726 g (1.29 mmol) of KOH, yielding a flaky, white paste (0.410 g, 75%). IR (COO^-): 1567, 1410 cm^{-1} . Anal. Calcd for $\text{C}_{26}\text{H}_{41}\text{O}_2\text{K}$: C, 73.53; H, 9.73; K, 9.21. Found: C, 70.76; H, 9.78; K, 9.33.

Cobalt(II) *p*-Styrylundecanoate (5) (General Procedure for Metal Exchange). In a 250-mL Erlenmeyer flask, 0.188 g (0.646 mmol) of cobalt(II) nitrate hexahydrate was dissolved in ethanol (10 mL) and water (10 mL). The solution rapidly became dull, pale red. An ethanolic solution of compound **2** (1.29 mmol) was prepared as above and slowly added dropwise with vigorous stirring into the cobalt chloride solution. As the addition proceeded, the solution became cloudy, and a deep purple precipitate formed. After the addition was complete, the mixture was heated gently for 5 min and allowed to cool. The mixture became clearer, the dark purple product having accumulated on the stirbar and the bottom of the flask. The final mixture was poured into a 250-mL separatory funnel, and the reaction flask was washed with pentane (2×30 mL). The purple organic layer was separated, and the colorless aqueous layer was extracted with pentane (2×20 mL). The combined organic layers were washed with a saturated aqueous NaCl solution (50 mL) and then deionized water (50 mL) and dried over anhydrous sodium sulfate. The solvents were removed in vacuo, yielding a tacky, dark purple solid (0.405 g, 76%). IR (COO^-): 1558, 1418 cm^{-1} . Anal. Calcd for $\text{C}_{52}\text{H}_{82}\text{O}_4\text{Co}$: C, 75.24; H, 9.96; Co, 7.11. Found: C, 74.21; H, 10.23; Co, 7.31.

Calcium *p*-styryloctadecanoate (4) was prepared by ion exchange from 0.153 g (0.646 mmol) of calcium nitrate tetrahydrate, yielding a dry, white solid (0.321 g, 61%). IR (COO^-): 1558, 1418 cm^{-1} . Anal. Calcd for $\text{C}_{52}\text{H}_{82}\text{O}_4\text{Ca}$: C, 76.98; H, 10.19; Ca, 4.94. Found: C, 75.03; H, 10.22; Ca, 4.50.

Manganese(II) *p*-styrylundecanoate (6) was prepared by ion exchange from 0.128 g (0.646 mmol) of manganese(II) chloride tetrahydrate, yielding a sticky, brown paste (0.361 g, 68%). IR (COO^-): 1557, 1418 cm^{-1} . Anal. Calcd for $\text{C}_{52}\text{H}_{82}\text{O}_4\text{Mn}$: C, 75.60; H, 10.00; Mn, 6.65. Found: C, 75.3; H, 10.24; Mn, 6.82.

Cadmium *p*-styrylundecanoate (7) was prepared by ion exchange from 0.119 g (0.646 mmol) of cadmium(II) chloride, yielding a white paste (0.475 g, 83%). IR (COO^-): 1545, 1418 cm^{-1} . Anal. Calcd for $\text{C}_{52}\text{H}_{82}\text{O}_4\text{Cd}$: C, 70.68; H, 9.35; Cd, 12.72. Found: C, 70.92; H, 9.70; Cd, 9.14.

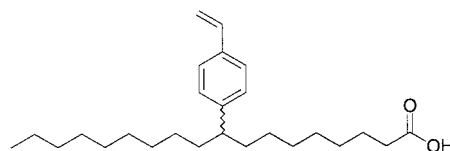
Copper(II) *p*-styrylundecanoate (8) was prepared by ion exchange from 0.129 g (0.646 mmol) of copper(II) acetate monohydrate, yielding a highly viscous, blue paste (0.456 g, 84%). IR (COO^-): 1586, 1418 cm^{-1} . Anal. Calcd for $\text{C}_{52}\text{H}_{82}\text{O}_4\text{Cu}$: C, 74.82; H, 9.90; Cu, 7.61. Found: C, 73.48; H, 10.15; Cu, 8.38.

Preparation and Polymerization of LC Samples. For all samples, 2-hydroxy-2-methylpropiophenone was used as an organic-soluble photoinitiator, and divinylbenzene was used as a cross-linking agent. For all salts, except copper ones, polymerization samples were prepared with the following composition (in terms of weight percent): metallomesogen,

87%; water, 7%; divinylbenzene, 5%; initiator, 1%. For monomer **8**, the following composition was used: metallomesogen, 93.5%; divinylbenzene, 5%; initiator, 1%; water, 0.5%.

Polymerizable LLC samples were prepared by first placing the desired amount of monomer and additives in a 40-mL centrifuge tube and mixing by hand. The samples were then alternatively centrifuged for 30 min at 2600 rpm and then sonicated for 15 min. This cycle was repeated three times. The samples were then allowed to stand undisturbed for 2 h. Photopolymerizations were carried out under light N_2 flush over a period of 6 h at ambient temperature (22 °C) using 365 nm irradiation. The light flux at the sample surface during photolysis was 1800 $\mu\text{W}/\text{cm}^2$.

Preparation of a CdS Nanocomposite. A thin-film sample of the inverted hexagonal phase of **7** was prepared and polymerized on a quartz plate. The sample was exposed to H_2S vapor in an enclosed chamber with an outlet. The H_2S vapor was generated from the neutralization of a saturated solution of sodium sulfide with 6 M sulfuric acid. The vapor generated was passed sequentially through a saturated potassium permanganate solution and a sodium hypochlorite solution acting as a scrubbing system.



Results and Discussion

p-Styryloctadecanoic acid, **1**, one of the parent monomers used in our previous works, exists as a mixture of regioisomers readily prepared from methyl phenylstearate.^{28–30} Sodium *p*-styryloctadecanoate, **2**, was previously found to exhibit broad inverse hexagonal lyotropic mesophasic behavior at room temperature. It also exhibits high compatibility with additional hydrophilic components and is thus well-suited for use in forming the LLC template. Several analogues of mesogen **2** were prepared by ion-exchange to explore the effects of different metal counterions on the mesophase behavior. Potassium *p*-styryloctadecanoate, **3**, was prepared by direct neutralization of acid **1** with KOH. Preparation of the calcium salt **4** and the transition-metal analogues was readily accomplished by the reaction of **2** with the appropriate water-soluble metal chloride, nitrate, or acetate in an aqueous/ethanolic environment. The sodium and potassium salts are freely soluble in the ethanolic solution, while the remaining salts are readily extracted into *n*-pentane, dried over sodium sulfate, and isolated from the solvent.

The presence and identity of mesophases formed by the neat salts were determined by low-angle X-ray diffraction (Table 1). Hexagonally arranged, indefinitely long columns display a characteristic set of *d*-spacings in the diffraction spectrum (Figure 1) with the ratio $1:\sqrt{3}:\sqrt{4}:\sqrt{7}:\sqrt{9}:\sqrt{12}:\dots$,³¹ while lamellar systems yield a spacing ratio of $1:\frac{1}{2}:\frac{1}{3}:\frac{1}{4}:\dots$. As previously observed, the neat sodium salt exhibited a very clear hexagonal mesophase at ambient temperature, wherein the first eight orders of diffraction could be observed (Figure 2).

(28) Harrison, W. J.; McDonald, M. P.; Tiddy, G. J. T. *J. Phys. Chem.* **1991**, *95*, 4136.

(29) Smith, F. D.; Stirton, A. J. *J. Am. Oil. Chem. Soc.* **1971**, *48*, 160.

(30) Smith, F. D.; Kenney, H. E.; Stirton, A. J. *J. Org. Chem.* **1965**, *30*, 885.

(31) Oster, G.; Riley, D. P. *Acta Crystallogr.* **1952**, *5*, 272.

Table 1. X-ray Diffraction Data for the Neat Salts of Monomer 1

counterion	phase ^a	d_{100} ^b	d_{110}	d_{200}	d_{210}	d_{300}	ICD ^c	color
sodium, 2	IH	36.2	20.9	18.3	13.6	12.2	41.9	white
potassium, 3	L	37.2	19.6	13.2	9.91	7.94	38.9	white
calcium, 4	IH	31.9	18.4	16.2	12.0		36.8	pale white
cobalt(II), 5	IH	29.6	17.3	15.0	11.4	10.1	34.5	violet
manganese(II), 6	IH	29.0	17.0	14.7	11.1		33.8	brown
cadmium, 7	IH	30.0	17.1	15.0	11.3	10.2	34.4	white
copper(II), 8	CH	22.6	13.2	11.5			26.3	dark blue

^a L, lamellar; IH, inverse hexagonal; CH, columnar hexagonal. ^b All distances are in angstroms. ^c Interchannel distance between structural units (columns or layers); values listed calculated by averaging data for first four reflections.

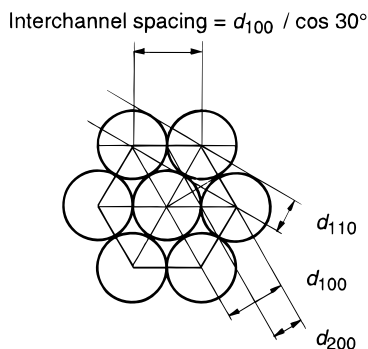


Figure 1. Representation of the first three X-ray diffraction planes in a hexagonal array of cylinders (i.e., a hexagonal mesophase).

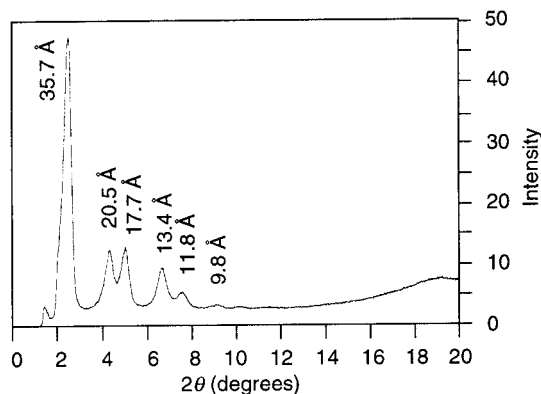


Figure 2. Low-angle X-ray diffraction profile of the polymerized inverted hexagonal phase of sodium salt **2**.

The interchannel spacing for hexagonal systems can be calculated from the primary diffraction peak, d_{100} , by simply dividing by a factor of $\cos 30^\circ$. For the neat sodium salt, the interchannel spacing was found to be 41.9 Å. The neat potassium salt, which has a counterion of equivalent charge but larger size, was found to form a lamellar phase at room temperature, with an interlayer spacing of 38.9 Å. Conversely, lithium phenylstearate, a closely related analogue with a smaller counterion, has been found to exhibit the inverse hexagonal phase at room temperature.³² This trend in phase behavior is consistent with the predictions of the critical packing parameter, where larger headgroups of equivalent charge favor the formation of lamellar or regular hexagonal phases.²¹

As can be seen in Table 1, a significant contraction was observed in the dimensions of the inverted hexagonal mesophase formed by neat samples of amphiphiles with metal ions of higher positive charge. Calcium *p*-styryloctadecanoate, **4**, formed an inverse hexagonal

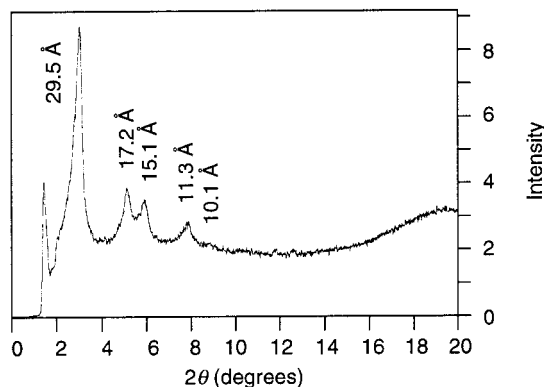


Figure 3. Low-angle X-ray diffraction profile of the inverted hexagonal phase of cadmium salt **7**.

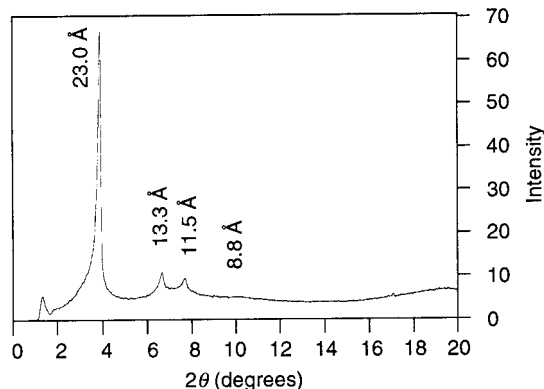


Figure 4. Low-angle X-ray diffraction profile of the columnar hexagonal phase of copper salt **8**.

phase with an interchannel spacing of 36.8 Å, smaller than the spacing for sodium analogue **2**. The cobalt(II), manganese(II), and cadmium(II) salts (**5**, **6**, and **7**, respectively) also formed inverse hexagonal phases, but with interchannel spacings slightly smaller than that of the calcium salt. In contrast, the dimensions of the mesophase formed by the copper(II) salt were significantly smaller than the other salts (cf. Figures 2–4).

Hexagonal diffraction spacings are characteristic of both inverse hexagonal lyotropic mesophases and columnar hexagonal thermotropic mesophases. Columnar mesophases have been found in metallophthalocyanines³³ and metal–crown ether assemblies.³⁴ Several transition metals, including molybdenum,^{35,36} chro-

(33) Piechocki, C.; Simon, J.; Skoulios, A.; Guillon, D.; Weber, P. *J. Am. Chem. Soc.* **1982**, *104*, 5245.

(34) Percec, V.; Heck, J.; Johansson, G.; Tomazos, D.; Kawasumi, M.; Chu, P.; Ungar, G. *J. Macromol. Sci. Pure Appl. Chem.* **1994**, *A31*, 1719.

(35) Baxter, D. V.; Cayton, R. H.; Chisholm, M. H.; Huffman, J. C.; Putilina, E. F.; Tagg, S. L.; Wesemann, J. L.; Zwanziger, J. W.; Darrington, F. D. *J. Am. Chem. Soc.* **1994**, *116*, 4551.

(32) Barron, C.; Spells, S. J. *J. Phys. Chem.* **1993**, *97*, 6737.

mium, copper,^{37,38} and rhodium³⁹ are known to form strongly coordinating dimeric species bridged by four carboxylates. These dimers also can assemble into hexagonal columnar phases, with intercolumn spacings smaller than those generally observed in inverse hexagonal lyotropic systems. Polarized light microscopy of the neat copper salt **8** and manipulation of the bulk material showed that **8** differed from the other transition-metal salts. The addition of water to a mixture containing copper salt **8** disrupted the pattern observed in the X-ray diffraction spectrum, whereas addition of water to the other salts only slightly modulated the dimensions of the phase. These observations are consistent with **8** exhibiting a thermotropic columnar hexagonal mesophase, rather than an lyotropic mesophase.

Infrared spectroscopy has previously been used to investigate the nature of the interaction in metal-carboxylate systems.⁴⁰ In such studies, the difference in energy between the symmetric and asymmetric stretching bands of the carboxylate group was related to the mode of association between the carboxylate and the metal center. However, the trends are only guidelines, since two different coordination modes often exhibit similar separations in the positions of the carboxylate bands. No clear correlation was observed between the splitting of the carboxylate bands of the salts prepared in the present work and the identity of the metal ion present. The only noticeable difference in the FT-IR spectra of the salts was that the carboxylate stretching bands of copper salt **8** appeared at much higher wavenumbers than those of the other salts (see the Experimental Section). This large shift may correspond to the tighter bidentate bridging observed in such copper carboxylate dimers.

Polymerization studies were conducted on mixtures of the metallomesogens to ensure that the structure of the mesophase was retained upon cross-linking. Since mesogen **2** and its derivatives only contain one polymerizable group, divinylbenzene was added to generate a heavily cross-linked network. The addition of water, divinylbenzene, and the photoinitiator to the LLC caused a variation in the dimensions of the mesophase. Since mass percentages were used in the preparation of the mixtures, the molar concentration of the additives present in the samples differed slightly depending on the identity of the counterion. However, the molecular mass of the mesogen is predominantly determined by the mass of the organic portion of the molecule. Additionally, preliminary studies of the sodium and potassium salts revealed that slight variations in the concentration of water or other additives (1–2 wt %) do not appreciably alter the dimensions observed for the overall mesophase.⁴¹

Photopolymerization of the LC mixtures was performed by exposing thin films of the samples to 365 nm

Table 2. X-ray Diffraction Data for Unpolymerized Mixtures of LC Salts of Monomer 1^a

counterion	phase ^b	d_{100}^c	d_{110}	d_{200}	d_{210}	d_{300}	ICD ^d
sodium, 2	IH	36.7	21.1	18.3	13.7	12.1	42.1
potassium, 3	L	38.2	19.5	13.0			38.8
calcium, 4	IH	30.9	18.1	15.7	11.9		36.1
cobalt(II), 5	IH	27.7	15.9	13.8	10.4		31.9
manganese(II), 6	IH	28.9	16.9	14.6	11.1	9.77	33.6
cadmium, 7	IH	30.0	17.4	15.3	11.5	10.2	34.9
copper(II), 8	CH	23.0	13.3	11.5	8.76		26.7

^a Composition for mixtures of monomers **2** through **7** (percent by mass): monomer, 87%; divinylbenzene, 7%; water, 5%; 2-hydroxy-2-methylpropiophenone, 1%. Composition for polymerization mixture of **8** (percent by weight): monomer, 93.5%; divinylbenzene, 5%; 2-hydroxy-2-methylpropiophenone, 1%; water, 0.5%. ^b L, lamellar; IH, inverse hexagonal; CH, columnar hexagonal. ^c All distances are in angstroms. ^d Interchannel distance between structural units (columns or layers); values listed calculated by averaging data for the first four reflections.

Table 3. X-ray Diffraction Data for Cross-Linked Phases of LC Salts of Monomer 1^a

counterion	phase ^b	d_{100}^c	d_{110}	d_{200}	d_{210}	d_{300}	ICD ^d
sodium, 2	IH	35.7	20.5	17.7	13.4	11.6	41.0
potassium, 3	L	38.2	19.2	13.0			38.6
calcium, 4	IH	30.4	17.7	15.4	11.6		35.4
cobalt(II), 5	IH	28.2	15.6	13.6	10.1	8.90	31.5
manganese(II), 6	IH	28.1	16.5	14.2	10.8	9.63	32.9
cadmium, 7	IH	29.5	17.2	15.1	11.3	10.1	34.5
copper(II), 8	CH	22.6	13.1	11.4	8.63		26.2

^a Composition for mixtures of monomers **2** through **7** (percent by mass): monomer, 87%; divinylbenzene, 7%; water, 5%; 2-hydroxy-2-methylpropiophenone, 1%. Composition for polymerization mixture of **8** (percent by weight): monomer, 93.5%; divinylbenzene, 5%; 2-hydroxy-2-methylpropiophenone, 1%; water, 0.5%. ^b L, lamellar; IH, inverse hexagonal; CH, columnar hexagonal. ^c All distances are in angstroms. ^d Interchannel distance between structural units (columns or layers); values listed calculated by averaging data for the first four reflections.

UV light. Each of the salts, excluding copper salt **8**, turned from a sticky, manipulable paste into a smooth, brittle solid. Polymerization of monomer **8**, on the other hand, caused the mixture to become more viscous, without forming a brittle solid. This behavior may arise from the difference in the packing of mesogens in lyotropic versus thermotropic discotic mesophases.

Inspection of the X-ray diffraction data for both unpolymerized and polymerized sample mixtures (Tables 2 and 3) shows that photopolymerization occurs with retention of the LC phase microstructure. It had been previously noted that in some samples, especially those with high divinylbenzene content, the sharpness of the diffraction peaks observed in the polymerized samples was blunted compared to the unpolymerized samples. Additionally, the unit cell dimensions of the hexagonal mesophases of each salt contracted slightly upon photopolymerization. Both observations are consistent with the formation of a highly cross-linked network, in which the disparate chains are drawn together, away from their original configuration, resulting in a small decrease in the organic volume. A high degree of polymerization in these systems was confirmed by the disappearance of FT-IR bands at 902 and 988 cm⁻¹, which are attributed to the reactive vinyl groups.

To demonstrate the ability of the polymerized lyotropic metallomesogens to function as templates for forming nanocomposite materials, the polymerized cadmium

(36) Cayton, R. H.; Chisholm, M. H.; Darrington, F. D. *Angew. Chem., Int. Ed. Engl.* **1990**, *29*, 1481.

(37) Ibn-Elhaj, M.; Guillon, D.; Skoulios, A.; Giroud-Godquin, A.-M.; Maldivi, P. *Liq. Cryst.* **1992**, *11*, 731.

(38) Chisholm, M. H.; Mackley, M. R.; Marshall, R. T. J.; Putilina, E. F. *Chem. Mater.* **1995**, *7*, 1938.

(39) Giroud-Godquin, A.-M.; Marchon, J.-C.; Guillon, D.; Skoulios, A. *J. Phys. Chem.* **1986**, *90*, 5503.

(40) Deacon, G. B.; Phillips, R. J. *Coord. Chem. Rev.* **1980**, *33*, 227.

(41) Unpublished results.

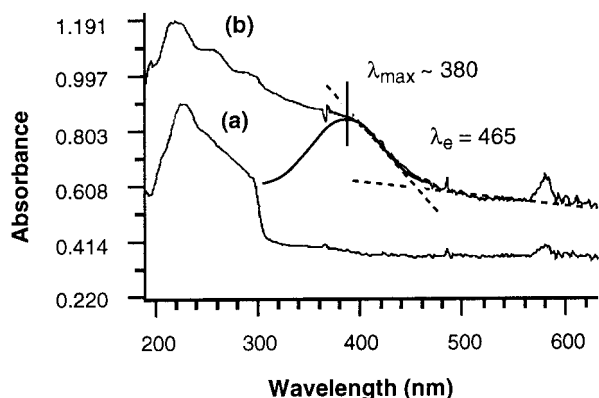


Figure 5. UV-visible absorption spectra of (a) the polymerized inverted hexagonal phase of cadmium salt **7** and (b) the polymerized cadmium network after exposure to H₂S vapor.

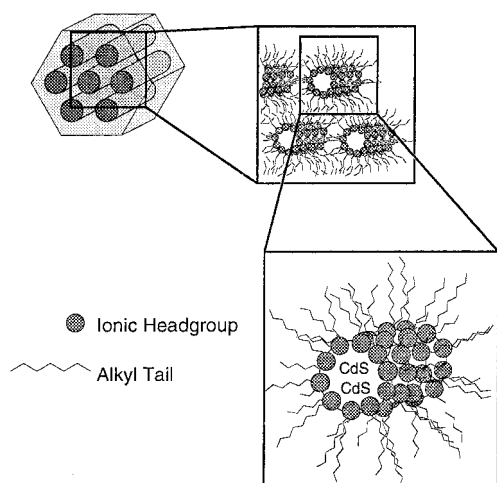


Figure 6. Formation of CdS particles within a liquid-crystalline template.

salt **7** was used to produce CdS nanoparticles within the hydrophilic channels (Figure 6). Cadmium sulfide can be precipitated by exposing a material containing Cd²⁺ ions to H₂S vapor. This method has previously been used to produce CdS particles in conventional polymer matrices,^{42–44} block copolymer systems,^{45,46} and different phases of nonpolymerizable amphiphile assemblies.^{47,48} The polymerized inverted hexagonal phase

of **7** was exposed to H₂S for 1 h, during which time the sample turned from white to dark yellow in color. Preliminary UV-visible characterization of the resulting composite revealed the presence of a new broad absorption band with an absorption maximum (λ_{\max}) at approximately 380 nm and an absorption threshold (λ_e) at 465 nm (Figure 5). These features of the UV-visible profiles of CdS nanoparticles have been correlated to the particle size and size distribution.^{49,50} On the basis of the more well-defined λ_e value observed, particle sizes with diameters of 40 Å or less were formed within the polymer matrix in this initial experiment. IR analysis of the composite also revealed a shift in the monomer carboxylate C=O stretching band from 1558 to 1708 cm⁻¹ after exposure to H₂S. This shift in carboxylate band position is consistent with a change in the coordination environment of the carboxylate groups, as would be expected with the loss of coordinated Cd²⁺ ions and subsequent protonation of the carboxylates upon CdS precipitation.

Low-angle X-ray diffraction revealed that the polymerized matrix was also less ordered after exposure to H₂S, possibly due to the loss of coordinated Cd²⁺ ions and protonation of the headgroups. We are currently investigating the properties of this nanostructured CdS composite and optimizing H₂S delivery conditions to determine if CdS particle size and distribution can be controlled with the aid of the ordered template.

Conclusion

A series of polymerizable transition-metal-containing amphiphiles has been prepared. Several of these mesogens form inverse hexagonal lyotropic phases that retain their structure after photopolymerization. We have shown that these mesogens provide an easy means for (1) modulating the dimensions of the inverted hexagonal phase and (2) providing a basis for synthesizing new inorganic materials within the hydrophilic channels of the template. In addition, the presence of the transition-metal ions may allow for the incorporation new properties into the nanocomposites.

Acknowledgment. Financial support from the National Science Foundation through a Faculty Early Career Development Award (DMR-9625433) is gratefully acknowledged. D.L.G. also thanks the 3M Company for an Untenured Faculty Award, and the Raychem Corporation and the Exxon Education Fund for research gifts.

CM970830K

- (42) Nelson, E. J.; Samulski, E. T. *Mater. Sci. Eng.* **1995**, *C2*, 133.
 (43) Moffitt, M.; Eisenberg, A. *Chem. Mater.* **1995**, *7*, 1178.
 (44) Moffitt, M.; McMahon, L.; Pessel, V.; Eisenberg, A. *Chem. Mater.* **1995**, *7*, 1185.
 (45) Yue, J.; Cohen, R. E. *Supramol. Sci.* **1994**, *1*, 117.
 (46) Kane, R. S.; Cohen, R. E.; Silbey, R. *Chem. Mater.* **1996**, *8*, 1919.
 (47) Braun, P. V.; Osenar, P.; Stupp, S. I. *Nature* **1996**, *380*, 325.
 (48) Tohver, V.; Braun, P. V.; Pralle, M. U.; Stupp, S. I. *Chem. Mater.* **1997**, *9*, 1495.

- (49) Lippens, P. E.; Lannoo, M. *Phys. Rev. B.* **1989**, *39*, 10935.
 (50) Spanhel, L.; Haase, M.; Weller, H.; Henglein, A. *J. Am. Chem. Soc.* **1987**, *109*, 5649.